EFFECTS OF FINITE WALL CONDUCTIVITY ON FLOW STRUCTURES IN NATURAL CONVECTION

E. Leonardi[1], T.A. Kowalewski[2], V. Timchenko[1], G. de Vahl Davis[1]

[1]University of New South Wales, Sydney, Australia 2052

[2]IPPT PAN, Polish Academy of Sciences, PL 00-049 Warsaw, Poland

ABSTRACT

Natural convection in a box is driven by the thermal boundary conditions at the active walls and is profoundly affected by the thermal conditions at the passive walls. The effects of these conditions were studied numerically and compared with experiments for natural convection in two cavities. The results indicate the importance of these conditions for proper modelling of three-dimensional flow structures, and also their inevitable influence on the Nusselt number.

INTRODUCTION

In the past, computational limitations have enforced several simplifications in the numerical modelling of thermally driven flows. One of the common misconceptions usually found is related to the thermal boundary conditions at the so called "side walls" of a box in which natural convection is occurring, *i.e.* walls which are not active in generating the flow, but simply play the role of a boundary for the flow domain. To simplify the problem, either adiabatic or perfectly conducting walls can be specified, or a specified heat flux can be imposed. However, this approach in many cases leads to solutions which are only approximately similar to the observed physical situations. On the one hand, this creates doubts about the quality of the numerical solutions, and on the other, is a serious obstacle in using experimental results for code validation and improvement.

Our previous investigations (Hiller *et al.* 1989,1990) have shown that gentle natural convection flows can be extraordinarily sensitive to small changes in the thermal boundary conditions. This is reflected in the results of numerical simulations, which show a similar sensitivity, and it is not easy to formulate proper mathematical boundary conditions to mimic those found in the laboratory.

Having this in mind, in this paper we describe our numerical and experimental attempts to understand and properly describe changes appearing in the flow structure due to the finite conductivity of both passive [nominally adiabatic] and active [heated or cooled] walls. It is worth noting that these are mainly three-dimensional variations of the flow patterns (a fact which perhaps partly excuses those who use classical two-dimensional programmes).

PROBLEM FORMULATION

We consider natural convection in two configurations: a horizontal temperature gradient in a side wall heated cavity, and a vertical temperature gradient in a lid cooled cavity.

The first configuration comprises low Rayleigh number natural convection in a cubical cavity with differentially heated active side walls. Two opposite vertical walls were isothermal and kept at temperatures T_h and T_c; the other four walls were passive: nominally insulators of finite thermal diffusivity. A heat flux, both through and along the walls, was generated due to temperature gradients existing between the fluid inside the cavity and the surrounding environment and also along the front and back walls, the lid and the floor of the box.

In the second configuration, the top wall of the cube was isothermal at a low temperature T_c. The other five walls were non-adiabatic, allowing a heat flux to cross from the external fluid surrounding the box. The temperature T_h of the external bath was kept constant. Due to forced convection in the bath it could be assumed that the temperature at the *external* surfaces of the box was close to the bath temperature. The temperature field at the inner surfaces of the walls adjusted itself depending on both the flow inside the box and the heat flux through and along the walls. Both configurations were used here to investigate the convective flow without phase change (and have previously been used to study the freezing of water at the cold wall, Kowalewski & Rebow 1998).

Experimental Set-up

A typical experimental set-up used to acquire temperature and velocity fields consisted of the convection box, a xenon flash or halogen tube lamp, and a CCD colour camera. Most of the experiments described here were performed using a cube-shaped cavity of 38 mm inner dimension. Either the two active vertical walls, or the active top wall were made of a black anodised metal to maintain isothermal boundary conditions. The remaining walls were made of 6 mm Plexiglas or 2 mm glass. The temperature of the isothermal walls was controlled by thermostats. As flow media, pure glycerine, its aqueous solutions and pure water were used. By varying the liquid composition and the temperature difference $\Delta T = T_h - T_c$, it was possible to cover a relatively wide range of Rayleigh and

Prandtl numbers (Ra = 2.10^4 - 3.10^6, Pr = 7-6900). The flow was observed at the vertical and horizontal cross sections of the cavity using a light sheet technique. The details of the experimental setup have been given elsewhere (Kowalewski *et al.* 1997, 1998).

Thermochromic liquid crystals (*TLC*) suspended in the working fluid were used both as flow tracers and temperature indicators. The computational analysis of the colour and displacement of the liquid crystal tracers allows us to determine both the temperature and velocity fields of the flow. It combines Digital Particle Image Thermometry (*DPIT*) and Digital Particle Image Velocimetry (*DPIV*) (Kowalewski *et al.* 1998). To obtain a general view of the flow pattern, several images recorded periodically within a given time interval were added in the computer memory, generating particle tracks.

Numerical method

A numerical simulation of the problem was performed using a three-dimensional finite difference vorticity-vector potential formulation of the Navier-Stokes and energy equations for laminar flow of a viscous, incompressible fluid. Solutions were obtained for Cartesian coordinates with the origin placed at a lower corner of the box. The *x*-axis is horizontal, the *y*-axis points upward and the *z*-axis is perpendicular to the active vertical plane. Modified versions of the FRECON3V (Timchenko *et al.* 1997) false transient solver have been used for the analysis of steady convection. To study transient convection with phase change a modified version of the code FREEZE3D (Yeoh 1993) was used. The computational models were adapted to simulate as closely as possible the physical experiment.

The main problem which arises in the simulation of experimental conditions is the proper definition of thermal boundary conditions (*TBC*). Either two opposite vertical walls or the horizontal top wall were assumed to be isothermal. Two approaches have been used to apply TBCs to the remaining walls, which are in reality neither adiabatic nor isothermal. In gthe first approach, TBCs were estimated by using heat transfer theory applied to a thick, infinitely wide plane plate of uniform conductivity exposed to an external constant temperature environment. In this one-dimensional approach, an arbitrary fixed temperature, a specific heat flux or a specific heat transfer coefficient on each of the six surfaces of the box wasimposed in the calculations. The general form of non-dimensional conditions used for the temperature θ at the boundary is:

$$A \cdot \theta + B \frac{\partial \theta}{\partial n} = C \qquad (1)$$

The constants *A, B* and *C* were calculated from the physical properties of the fluid, the wall materials and a specified heat transfer coefficient *h*. By setting *A* and *C* to zero, adiabatic *TBC*s are obtained. To set isothermal or mixed thermal boundary conditions, *A* is set to 1, and *C* is equal to the non-dimensional external temperature θ_∞. Then, *B* can be found from:

$$B = -\frac{k_l}{hL}\left[1 + \frac{hd}{k_w}\right] \qquad (2)$$

where *L* and *d* are the cavity height and wall thickness, while k_w, and k_l are the thermal conductivities of the wall and liquid respectively.

In the second approach, by incorporating all walls bounding the flow in the computational domain, a coupled solid-fluid conjugate heat transfer problem is solved (3-D *TBC).* Now equation (1) is applied to set *TBC*s at the external surfaces of the walls, *i.e.* to specify a heat flux at *the external surfaces of the walls*. By setting constants *A=1*, C=θ_∞ in equation (1) and using an arbitrary specified heat transfer coefficient together with the wall thermal conductivity *B* simplifies to

$$B = -\frac{k_w}{hL}.$$

The effects of temperature-dependent fluid properties were also investigated by implementing appropriate functional relations for the viscosity, thermal conductivity, heat capacity and density of the fluid into the codes.

To check the validity of the numerical solution in comparison with the experimental results, several methods of numerical visualisation were applied. In the first step the general flow characteristics, such as the two-dimensional temperature and velocity fields, were extracted. A detailed visualisation of the calculated flow structures was achieved using particle tracks obtained through the integration of the velocity equations. Typical solutions were computed on a 31x31x31grid (with additional grid points in the solid phase, where appropriate), chosen as a compromise between accuracy and cost. It has been found that this mesh is more than adequate if only a global description of the flow is of interest. However, the localisation of singularities and the determination of fine, three-dimensional characteristics of the tracks such as the pitch of spirals, appeared to be more sensitive to the mesh size, especially at higher values of the Rayleigh number.

SELECTED RESULTS

Differentially heated cavity

Our general observation coming from the investigated flow systems is that *TBC*s imposed at the passive walls have a considerable effect on the three-dimensional flow structure. The main flow pattern usually remains predictable for any given imposed temperature gradient, and can, in general terms, be described using simple two-dimensional

modelling of the symmetry plane. However, three-dimensional modelling becomes sensitive to *TBC*s when the flow away from the symmetry plane is analysed. A good example of *TBC* effects is given by the standard double glazing problem investigated in the cube-shaped cavity. The flow is driven by the temperature difference between the vertical hot wall *(θ_h =1* at *x=0)* and the opposite cold wall *(θ_c =0* at *x =1).*

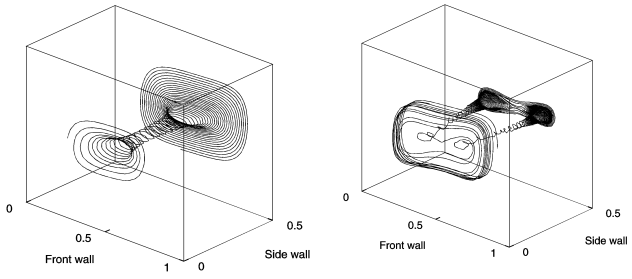

Case #1 case #11

Fig. 1. Calculated 3-D streamlines (front half of the cavity displayed only) for adiabatic *TBC* (case #1 and #11 in Table 1). One or two straight spirals run towards centre (case #1) or towards front wall (case #11).

The three-dimensional flow structure consists of one or two spiralling motions responsible, in addition to the main recirculation, for a cross-flow from the front and back walls to the cavity centre (Fig. 1). Initially our interest was directed towards understanding the flow in the vertical centre plane of the cavity. For this purpose the observations of flow patterns and temperature fields were performed for several systems with increasing Rayleigh numbers. Measured and calculated temperature and velocity fields have generally shown good agreement. The main flow, being responsible for the overall heat transfer, is well predictable and rather insensitive to *TBC*s at the side walls. However, in comparing details of the three-dimensional flow structure, several distinct discrepancies were found. At lower Rayleigh numbers (*Ra* =21,000), a computed single straight spiral transporting liquid from the front and back walls into the centre plane has, a different pitch compared with experiments (Hiller *et al.* 1989), and its ends are curved. At *Ra* = 80,000, the computed solution shows two rolls whereas in the experiment, only one spiral initially appears at the front and back walls. This splits midway along its length into two spirals forming characteristic 'cats eyes' in the symmetry plane. The direction of the observed inner spiral is in both cases towards the centre symmetry plane (compare Fig. 3 in Hiller *et al.* 1990).

Several numerical investigations have been performed to explore this effect. It seems that the *z*-component of the flow velocity responsible for the three-dimensional behaviour of the tracks is extremely sensitive to *TBC*s on all passive walls. Depending on the value and direction of the wall heat flux, the location of the core of the spirals at the side walls may be shifted towards the hot or cold side. In this way their pitch and even direction may be easily changed. Due to this sensitivity the estimation of the proper *TBC*s for the given experiment becomes a non-trivial task, especially for the two-roll system. The trial and error method first used to fit the *TBC*s was replaced by a process of defining an explicitly measured temperature distribution for all four non-isothermal walls. Both the direction of the calculated spirals and their pitch correlate well with the measured particle tracks (Hiller *et al.* 1992, Kowalewski *et al.* 1994). The improvement obtained gives an indication of the necessity of modifications to the modelling of heat transport through and along non-isothermal walls.

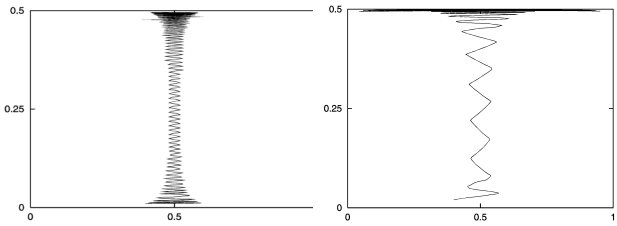

Case #1 Case #5

Fig. 2 Calculated streamlines in the horizontal centre plane (*y=0.5*) for adiabatic *TBC*. The tracks run from the front wall (bottom of the figures) to the cavity centre. Effect of the side wall thickness on a pitch of the tracks (case #1 and #5 in Table 1a).

Table 1a. Numerical results for Ra=21,000, Pr=6300.

Case	TBC				d/L	$\|U_{max}\|$	$\|V_{max}\|$	$\|W_{max}\|$	Nu_C	Nu_B
	#D	A	B	C					(X=0)	(Y=0)
#1	1D	0	1	0	0	24.26	30.09	2.182	2.76	0
#2	3D	0	1	0	0.067	25.25	30.77	2.839	2.59	0
#3	3D	0	1	0	0.167	26.21	31.49	3.378	2.49	0
#4	3D	0	1	0	0.3	26.83	31.92	3.648	2.43	0
#5	3D	0	1	0	0.5	27.12	32.12	3.756	2.41	0
#6	1D	1	4.04	0.5	0.157	24.54	30.26	2.250	2.76	0.052
#7	3D	1	2.56	0.5	0.167	26.35	31.56	3.385	2.49	0.290
#8	3D	1	2.56	0.5	0.5	27.13	32.13	3.750	2.41	0.403

Table 1b. Numerical results for Ra=80,000, Pr=6900.

Case	TBC				d/L	$\|U_{max}\|$	$\|V_{max}\|$	$\|W_{max}\|$	Nu_C	Nu_B
	#D	A	B	C					(X=0)	(Y=0)
#11	1D	0	1	0	0	40.96	62.94	5.307	4.41	0
#12	3D	0	1	0	0.067	42.68	64.66	7.316	4.15	0
#13	3D	0	1	0	0.167	44.28	66.38	8.971	4.00	0
#14	3D	0	1	0	0.3	45.24	67.47	9.820	3.93	0
#15	3D	0	1	0	0.5	45.68	68.12	10.20	3.89	0
#16	1D	1	4.04	0.5	0.157	41.33	63.32	5.566	4.39	0.061
#17	3D	1	2.56	0.5	0.167	44.44	66.55	9.050	3.99	0.405
#18	3D	1	2.56	0.5	0.5	45.70	68.15	10.20	3.89	0.548

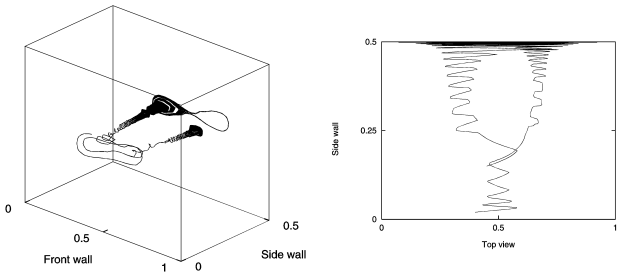

case #16 case #17

Fig. 3. Calculated streamlines for non-adiabatic *TBC* (case #16 and #17 in Table 1b). Right figure: *1-D TBCs* used, unable to predict observed splitting of the spirals. Additional saddle points close to the centre plane (y=0.35) divide the spirals into two, running in opposite directions; this was not observed in the experiments. Left figure: *3D-TBCs* correctly predict splitting of the spirals and their direction (to the centre).

To elucidate the effect of finite wall thickness, a series of numerical experiments using adiabatic and non-adiabatic *TBC*s was performed Some of the results are presented in Tables 1a and 1b. The tables show the variation of the maxima of the *x, y* and *z* velocity components, the average Nusselt number for *x = 0* (the hot active wall) and *y = 0* (the bottom passive wall). Adiabatic (first five cases) and non-adiabatic *TBC*s (last three cases) were simulated using both one-dimensional and three-dimensional wall conduction models. The parameters used for non-adiabatic *TBC* models correspond to the typical experimental conditions: convective heat transfer between 6 mm plexiglas wall and air (h = 2 W/m^{2}K). The outside air temperature is set to be equal to the mean temperature in the cavity ($C=\theta_\infty$=0.5). The Rayleigh and Prandtl numbers correspond to the typical experimental conditions for glycerine; the temperature differences were 4 K and 16 K, respectively, for the two values of *Ra*. In all simulations where three-dimensional *TBCs* were used, both active isothermal metal walls had a fixed non-dimensional thickness of 0.067 (2.5 mm). The temperature variation calculated at these walls was found to be negligibly small.

Several flow features are illustrated in the tables. It can be seen that although the main velocity components *U* and *V* remain rather insensitive to modifications of *TBC*, the cross flow distinctly varies (see also Fig. 2). This explains the previously observed discrepancies in the spiral pitch between numerical and experimental tracks (Hiller *et al.* 1989, 1990). It is worth noting that the effect of cross-flow variation is almost solely due to the finite wall thickness, and the influence of the additional heat flux through the non-adiabatic walls is very small. Obviously 1-D *TBC*s cannot be used to explain three-dimensional flow topology for this flow configuration, even if a proper set of non-adiabatic *TBC*s is used (see Fig. 3). The cross flow evidently decreases the mean heat flux through the cavity, as shown by the variation of Nusselt number Nu_C. The heat flux through the top/bottom walls (Nu_B) is almost one order of magnitude lower when a one-dimensional *TBC* model is used for non-adiabatic cases. Figure 4 illustrates the computed variation of isotherms calculated for the centre vertical cross-section of the cavity. It is interesting to note that despite distinct changes of the temperature fields, the calculated velocity profiles almost completely overlap for the investigated variations of the *TBC*.

In the above examples only symmetrical cases have been shown. In reality, the external temperature may deviate from the mean value. Numerical simulations performed for the two extreme cases, *i.e. C=0,* and *C=1*, have shown that this is the parameter responsible for the observed bending of the cross-flow spiral at *Ra* = 21,000 and for the asymmetry and the splitting of the spirals at *Ra* = 80,000. It is worth noting that only the three-dimensional *TBC* models predict the splitting of the spirals in a manner similar to that observed.

In all cases described above the effects of variable fluid properties appeared to be secondary compared with the effects of the *TBC*. In the next set of results pure water is used as a flow medium. This case is of particular interest because natural convection of water in the vicinity of the freezing point

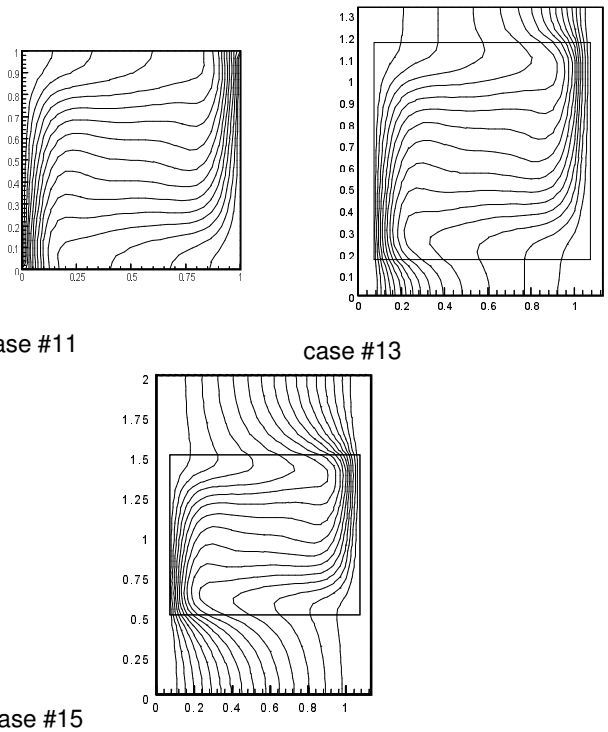

case #11 case #13

Case #15

Fig 4. Isotherms calculated for the centre plane (z=0.5); case #11, #13 and #15 in Table 1b. Effect of the side wall thickness for adiabatic TBC: *d/L=0* (left), *d/L=0.167* (right), *d/L=0.5* (bottom).

differs greatly from all normal cases due to the water density anomaly. In the investigated cases, for a hot wall temperature of *10 °C* and the cold wall at *0 °C,* the competing effects of positive and negative buoyancy forces, and the interacting layers of hot and cold liquid (Fig. 5), create an interesting flow pattern. Two main circulations are clearly visible: an upper clockwise circulation transporting hot liquid towards the top wall and back along the isotherm of the density extremum, and a lower counter-clockwise circulation within the cold region adjacent to the ice surface. At the cold wall, the descending hot liquid interacts with the rising cold liquid. This creates a distinct saddle point approximately at the wall mid height. Experiments show that this configuration is very sensitive to *TBC*s at the four passive walls. For example switching on or off the external air flow changes the position of the saddle point, shifting it from the lower part almost to the top of the wall. In the numerical model, a variation of *TBC* shows a similar sensitivity as illustrated in Fig. 5.

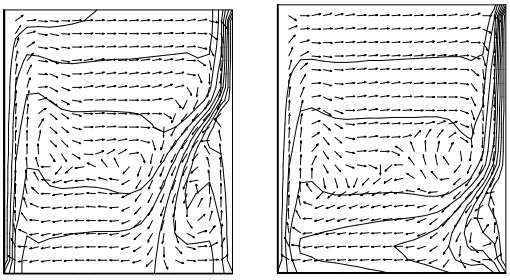

(a) (b)

Fig. 5. Natural convection of water, numerical results for T_h=10°C, T_c=0°C, Ra=1.5·10^6, Pr=13.3. Velocity and temperature fields in the centre plane (z=0.5). Effect of *TBC*; (a) - adiabatic, *1-D TBC,* (b) - non-adiabatic, *3D-TBC* with *d/L=0.167.*

In Figure 6 vertical velocity profiles extracted along the cold wall illustrate the strong dependence of the saddle point position on the heat flux through the side walls. The configuration of colliding cold and warm fluid layers has a direct influence on the heat transfer and determines the interface growth rate and its shape. The above mentioned sensitivity of the flow structure on *TBC*s can be responsible for distinct discrepancies between experimental and numerical results, reported for ice growing in the freezing of water (Kowalewski & Rebow 1998).

Lid cooled cavity

Natural convection in a cubical box immersed in a hot water bath and cooled from above has been extensively investigated for water, both with and without phase change. Here, due to the intense heat flux through the side walls, a proper modelling of the *TBC*s appears to be crucial for describing velocity and temperature fields in the centre symmetry plane as well as away from that plane.

The steady state flow exhibits a single downwards flowing cold jet along the vertical cavity axis and reversed upwards flow along the side walls. Flow visualisations (Kowalewski & Cybulski 1997) have shown the existence of a complex spiralling structure transporting fluid up the side walls and down in a central cold jet along the cavity axis. For walls of high heat conductivity (*e.g.,* glass), eight symmetric cells were created by the flow (Fig. 7). For Plexiglas walls, additional small recirculation regions appeared separating the main cells.

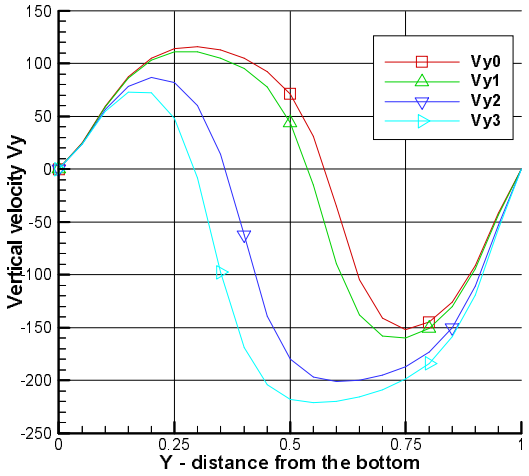

Fig. 6 Natural convection of water (parameters like Fig. 5). Vertical velocity profiles calculated close to the cold wall (vertical line at x=0.93, z=0.5) for 1D-TBC. Effect of the heat flux through the side walls: Vy0 - adiabatic, Vy1 - h=2W/Km^2, Vy2 - h=20W/Km^2, Vy3 - h=40W/Km^2. Zero crossing of the profiles indicates position of the saddle point of the colliding hot-cold circulations.

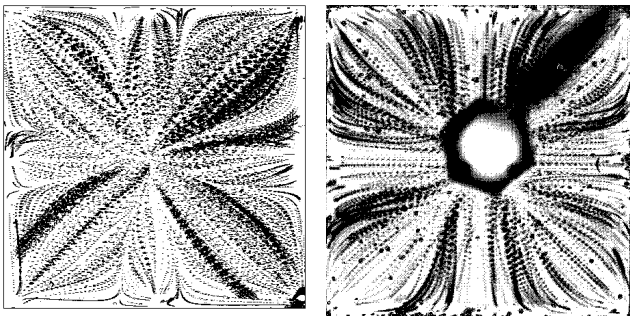

Plexiglas walls, *d=8mm* Glass side walls, *d=2mm*

Fig. 7 Natural convection of water in lid cooled cavity: T_h=21°C, T_c=15.5°C, Ra=2.7·10^6. Particle tracks observed underneath the lid for plexiglas (left) and glass (right) *passive* walls of the cavity.

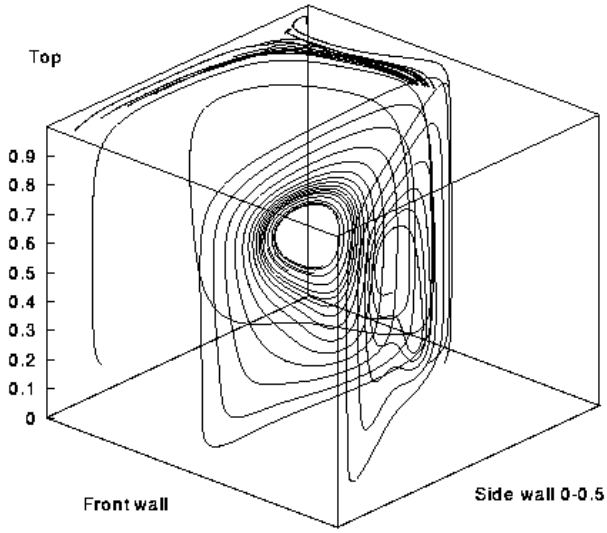

a) Plexiglas walls

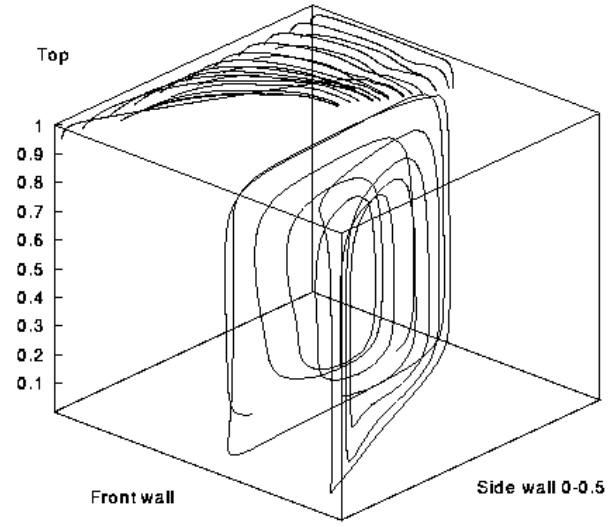

b) Glass walls

Fig. 8 Calculated three-dimensional streamlines in lid cooled cavity with plexiglas (a) and glass (b) *passive* walls. Numerical results obtained for *3-D TBC* and flow parameters corresponding to Fig. 7.

Although the computational results obtained for idealised one-dimensional *TBC*s confirmed the eight-fold symmetry of the temperature and flow fields observed experimentally, their orientation was different. Moreover, the measured isotherms were evidently shifted to higher values. Serious discrepancies were noticed for the temperature distribution observed at the horizontal cross-section.

In several computational runs using the one-dimensional *TBC* model the heat flux was step-wise modified to produce better agreement with the measured temperature profiles. It was found that such agreement could be obtained by assuming nearly twice as much heat flux through the side walls as the nominal value calculated from the physical characteristics of the side walls (Abegg *et al.* 1994).

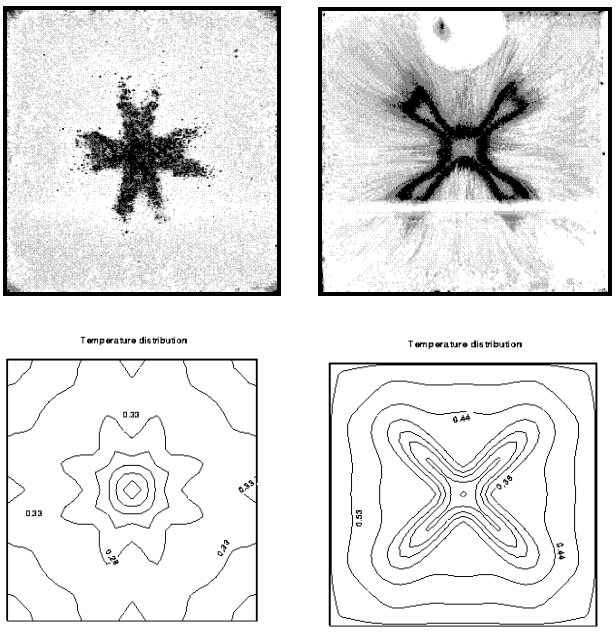

Plexiglas walls d = 8mm Glass side walls, d = 2mm

Fig. 9 Natural convection of water in lid cooled cavity: T_h=21°C, T_c=15.5°C, Ra=2.7 10^6. Temperature distribution underneath the isothermal lid (plane y=0.9); top row - experimental, temperature visualized with help of liquid crystals, bottom row numerical results for *3-D TBC.*

This indicates that the heat flux along the side walls, neglected in the simple one-dimensional model of the *TBC*, effectively increases the heat transfer from the external medium. The differences between the observed and calculated flow patterns remained even after such arbitrary modifications of the *TBC*s. Consequently, the calculated streamlines starting in the diagonal symmetry plane spiralled in the *opposite direction* to that observed in experiments. Especially for 8mm thick Plexiglas walls, *TBC*s could not be properly modelled using a one-dimensional heat flux assumption. Physically it is possible for a flow pattern with an opposite sequence to develop, that is spiralling inwards in the central plane and outwards on the diagonal plane. Therefore only a slight change of the *TBC*s may modify the flow pattern. This was observed by replacing the side walls of low conductivity Plexiglas by thin glass walls.

The numerical simulations performed for both cases using the three-dimensional model for wall conduction confirmed the triggering mechanism of *TBC*s on the observed flow pattern. Inclusion of the side walls in the computational domain and solving the coupled fluid-solid heat conduction problem considerably improved the agreement with the observed flow pattern (Fig. 8). The observed temperature distribution as well as its symmetry were correctly predicted in the numerical results (Fig. 9). As a result of using *both* the experimental and numerical methods, the fine structures of the thermal flow were fully understood.

CONCLUSIONS

Our investigations show that numerically calculated three-dimensional flow structures strongly depend on the modelling of the thermal boundary conditions at the *passive* side walls. This becomes important in simulating several practical situations, such as propagation of pollution, micro-segregation and aggregation of impurities in solidification. It also appears that modelling of *TBC*s has a noticeable influence on the overall heat flux, which is of interest in the design of heat exchangers or thermal insulation.

REFERENCES

Abegg, C., de Vahl Davis, G., Hiller, W.J., Koch, St., Kowalewski, T.A., Leonardi, E., Yeoh, G.H., 1994, Experimental and numerical study of three-dimensional natural convection and freezing in water; *Heat Transfer 1994,* vol. 4 , pp 1-6, G.F. Hewitt (eds.), IChemE.

Hiller, W.J., Koch, St., Kowalewski, T.A., 1989, Three-dimensional structures in laminar natural convection in a cube enclosure, *Exp. Therm. and Fluid Sci.*, vol.2, pp 34-44.

Hiller, W.J., Koch, St., Kowalewski, T.A., de Vahl Davis, G., Behnia, 1990, M., Experimental and numerical investigation of natural convection in a cube with two heated side walls, *Proc.of IUTAM Symposium,* Cambridge UK, Aug. 1989, (Edits. H.K. Moffat & A. Tsinober), pp 717 - 726, CUP 1990.

Hiller W.J., Koch, St., Kowalewski, T.A., Mitgau, P., Range, K., 1992, Visualization of 3-D natural convection, *Proceedings of The Sixth International Symposium on Flow Visualization,* Eds. Tanida Y. & Miyashiro H., pp 674-678, Springer-Verlag.

Kowalewski T.A., Cybulski A., Rebow. M., 1998, Particle Image Velocimetry and Thermometry in Freezing Water, in *8th Int. Symposium on Flow Visualization,* Sorrento, Sept. 1998, Edits. G.M. Carlomagno & I. Grant, CD ROM Proceedings ISBN 0953399109, p. 24.1-24.8, Edinburgh.

Kowalewski, T. A. Cybulski A., 1997, Natural convection with phase change (in Polish), *IPPT Reports* 8/1997, IPPT PAN Warszawa.

Kowalewski T.A., Hiller W.J., de Vahl Davis G, 1994, Computational and experimental visualisation in heat and mass transfer problems, in *Proc. of the First Japanese-Polish Joint Seminar in Advanced Computer Simulation*, Tokyo, Nov., 1993, Edts. Akiyama, Kleiber, Wolanski, pp. 60-69, University of Tokyo.

Kowalewski T.A., Rebow. M., 1998, Freezing of water in the differentially heated cubic cavity, *Int. J. of Comp. Fluid Dyn.* (in press).

Timchenko, V., Leonardi, E. and de Vahl Davis, G., 1997, FRECON3V Users' Manual, *The University of New South Wales, School of Mechanical and Manufacturing Engineering, Report 1997/FMT/1.*

Yeoh, G.H., 1993, Natural convection in a solidifying liquid, *Ph.D. Thesis*, University of New South Wales, Sydney.